Estimation of Harmonics in Partly Monitored Residential Distribution Networks With Unknown Parameters and Topology

Pablo Rodríguez-Pajarón, *Graduate Student Member, IEEE*, Araceli Hernández, *Member, IEEE*, and Jovica V. Milanović, *Fellow, IEEE*

***Abstract*—The generalized adoption of power-electronic-based loads in residential networks is leading to increasing concern about harmonic distortion levels. At the same time, residential distribution systems are insufficiently monitored to provide a reliable analysis of harmonic limits compliance at the point of common coupling of customers. To address this problem, this paper proposes a practical method to estimate voltage harmonic levels in real time at all connection points of residential consumers. The proposed methodology assumes unknown network parameters and topology according to the limited data availability which is usual in low voltage residential networks. The proposed harmonic estimation method uses information gathered from conventional smart meters typically installed in the network (which register fundamental voltage and power) and from a reduced number of installed power quality monitors. A penetration of power quality meters below 10% has proved to provide accurate estimations of voltage harmonic levels at the whole network. The paper also proposes a methodology to optimally locate these power quality meters in the network. Validation of the methodology is performed in two different European distribution test networks with 55 buses and 471 obtaining satisfactory results. The method's robustness and the parameters affecting accuracy are also analyzed in the article.**

***Index Terms*—Distribution network, harmonic distortion, power quality, probabilistic analysis, residential distribution system, unknown parameters.**

NOMENCLATURE

δ	Correlation threshold.
$\underline{\kappa}_{i,j}^{h}$	Equivalent radial impedance between buses i and j for order h.
$\boldsymbol{C}$	Correlation matrix.
$\boldsymbol{C_{bin}}$	Binary correlation matrix.
h	Harmonic order h.
I_k^h	Harmonic current of order h injected at bus k.
I_{ij}	Fundamental current between buses i and j.
P	Active power.
Q	Reactive power.
r	Real part of radial equivalent impedance.
$V_k^{(t)}$	Fundamental voltage at bus k and time t.
V_k^h	Harmonic voltage of order h at bus k.
x	Imaginary part of radial equivalent impedance.
$\boldsymbol{y}$	Monitor location binary array.

Manuscript received July 22, 2021; revised January 26, 2022; accepted February 25, 2022. Date of publication March 2, 2022; date of current version June 21, 2022. This work was supported by MCIN/AEI/10.13039/501100011033 under Grant RTI2018-097424-B-I00, and by "ERDF A way of making Europe." Paper no. TSG-01160-2021. *(Corresponding author: Pablo Rodríguez-Pajarón.)*

Pablo Rodríguez-Pajarón and Araceli Hernández are with the Escuela Técnica Superior de Ingenieros Industriales, Universidad Politécnica de Madrid, 28006 Madrid, Spain (e-mail: pablo.rpajaron@upm.es).

Jovica V. Milanović is with the Department of Electrical and Electronic Engineering, University of Manchester, Manchester M13 9PL, U.K.

Color versions of one or more figures in this article are available at https://doi.org/10.1109/TSG.2022.3155976.

Digital Object Identifier 10.1109/TSG.2022.3155976

I. INTRODUCTION

VOLTAGE harmonic distortion in residential distribution networks (RDN) is arousing increasing concern and interest from both, distribution system operators (DSO) and academia [1]–[6]. With the aim of improving efficiency and decarbonizing the economy, a generalized adoption of power-electronic-based devices has taken place in recent years in the residential sector, leading to an increase in voltage and current distortion levels [7], [8]. That is the case, for instance, of lighting, where conventional linear loads (i.e., incandescent lamps) have been massively replaced by compact fluorescent lamps (CFLs) and later by light-emitting diodes (LEDs) [9]. Also different motors of household appliances, such as washing machines or refrigerators, are being increasingly fed through variable speed drives (VSD) [2], [10].

Despite the increase in harmonic levels that is foreseen in a near future, and the potential threats that it may cause, the low voltage distribution network has two particularities that make the assessment of harmonic distortion complicated. First, these networks are usually poorly monitored [11]–[13] due to the associated costs; and, second, the network parameters and even topology are very frequently unknown [14], [15].

To overcome the first of the aforementioned difficulties, some of the past reports have proposed different harmonic state estimation (HSE) methods relying on using phasor measurement units [11], [16] or regular power quality (PQ) meters [12], [13], [17], and have analyzed their optimal location [18], [19]. None of these methods, however, overcome the second difficulty, i.e., the unavailability of network parameter data. In [20], uncertainty of network parameters is assumed, whilst some network information is required and the topology is supposed to be known.

In addition, previous HSE works typically estimate harmonic injections from historical data gathered from past measurement campaigns [12], [13], [21]. These past measurements may not be representative of present system loads if there have been changes in the devices connected to the system after the measurements were carried out. In comparison, the proposed method is based on a real time estimation of injected currents which is continuously updated and, therefore, considers the actual characteristics of loads connected at present.

In short, this work proposes a new practical and computationally non-intensive method to estimate voltage harmonics in residential networks with entirely unknown parameters and topology. The main contributions of the paper compared to the past works are as follows: i) The proposed methodology assumes that network parameters and network topology are unknown as it is commonly the case in LV residential grids. All the previous approaches existing in the literature for harmonic estimation consider the network parameters as known [11]–[13], which is very unusual in practice [14], [15]; ii) Only conventional smart meters (SM) (which measure power and fundamental voltages) installed at residences and a reduced number of PQ monitors (at about 10% of the buses) are necessary to obtain the harmonic estimation in the whole network. On the contrary, most of the previously reported methods have more restrictive monitoring requirements such as the need for expensive PMUs [11], [16]; iii) An optimization procedure is developed to minimize the number of PQ monitors in the network and to connect them to the most appropriate buses yielding full harmonic observability in the network.

The proposed methodology is computationally efficient (less than 2 sec of CPU time for near 500 bus network). It has been validated on two RDN using harmonic pseudo-measurements with stochastic characteristics to ensure representative scenarios. The key parameters affecting the performance of the method have been also assessed.

The paper is structured as follows: Section II shows an overview of the complete methodology. The algorithm to optimally locate PQ monitors is described in Section III and the method to estimate harmonic voltages is explained in Section IV. The strategy followed to validate the method and the results of its application are described in Section Vand VI. Finally, a discussion on the robustness and accuracy of the method is included in Section VII, followed by general conclusions.

II. Methodology Overview

The methodology proposed utilizes harmonic measurements collected at a reduced number of monitored buses in a residential LV network to estimate voltage distortion levels at all non-monitored locations. Network parameters and topology are not known in this method in accordance with the common practical approach in LV systems where network models are rarely available. The methodology assumes that consumer buses are equipped with a conventional meter, capable of recording active and reactive demand and fundamental voltage magnitude. In addition, a small number of PQ monitoring devices will be installed at certain buses. The number and location of these PQ meters will be further discussed in Section III. The required inputs of the method and the obtained output are schematically summarized in Fig. 1.

Fig. 1. Overview of the proposed methodology for estimating harmonic voltages.

The proposed methodology basically consists of two stages:

1) PQ monitor location. A reduced number of PQ monitors are installed at certain buses. The optimal location of these monitors is selected by means of the information provided by conventional consumers' meters. This stage is performed just once and the location is afterwards fixed for the rest of the estimation process. The number of available PQ monitors will determine the accuracy of the harmonic estimations. This stage is discussed in Section III.
2) Voltage harmonic estimation. With the information extracted from PQ monitors located according to Stage 1 and the data provided by conventional meters for the rest of consumers, harmonic voltages are estimated all over the network. This stage will be discussed in detail in Section IV.

III. PQ Monitor Location

To perform voltage harmonic estimation, it is convenient to determine first the optimal number and location of PQ meters. The aim of this stage of the method is finding such locations.

In order to find the optimal placement of PQ monitors, in this method the information provided by conventional SM (installed at every consumer bus) will be used. These meters (widely installed in today RDN) provide active and reactive power measurements as well as fundamental voltage magnitude [22], [23]. In particular, the voltage magnitude measurement will be a key parameter to establish groups of buses whose voltage levels are correlated at fundamental frequency. It has been found that these buses also show high correlation in harmonic voltage levels. This finding is supported by the fact that electrically close buses will have high correlation of respective fundamental voltages. These buses will also be electrically close for harmonics orders and, therefore, will be characterized by a high THD correlation provided that the currents injected in different residential buses have a similar distribution.

This idea is illustrated using a practical example in Fig. 2. In the right part of this figure, the correlation matrix between voltage total harmonic distortion (THD, computed up to 17^{th} harmonic order) values obtained at the 55-buses of the IEEE LV European test feeder [24] network is shown with a color map. Each term of this matrix shows the Pearson correlation factor between the series of THD values obtained during one week in 10-minute intervals at each pair of buses defined at each element of the matrix. For instance, element (1,2) of

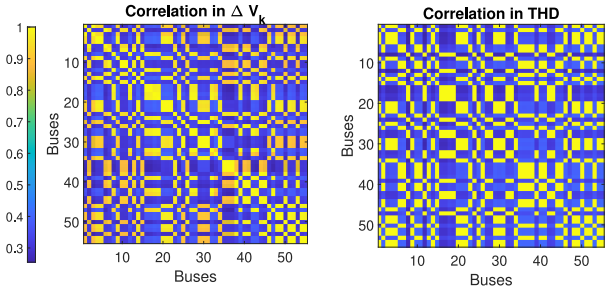

Fig. 2. Correlation matrices for ΔV_k (left) and THD (right).

the matrix on the right of Fig. 2 represents the correlation between the weekly voltage THD at buses 1 and 2. THD values have been estimated by considering simulations with stochastic harmonic injections (that vary randomly in time and from one customer to another) generated for each consumer using the procedure explained in detail in Section V-B. On the left, the figure shows the Pearson correlation matrix of ΔV_k obtained at each bus during the studied week in 10-minute intervals by using the same colour map. Parameter ΔV_k is defined as:

$$\Delta V_k = \left(V_0^t - V_k^t\right) - \left(V_0^{t+1} - V_k^{t+1}\right) \tag{1}$$

where V_0^t and V_0^{t+1} are the fundamental voltage values at the secondary of the main substation transformer at a certain time interval t and at the following one $t+1$; and V_k^t and V_k^{t+1} refer to the fundamental voltage at bus k at a certain time interval t and the next one $t+1$.

By observing Fig. 2, it can be seen that these two matrices present very similar colour maps or, in other words, buses with highly correlated ΔV_k also have highly correlated THD values. It is important to highlight that values of the matrix on the left, ΔV_k, are available just by measuring the fundamental voltages, i.e., with conventional SM.

The basic idea of this monitor location method relies on placing a PQ monitor in each group of buses with high THD correlation among them. Considering the properties explained and illustrated in Fig. 2, buses with high THD correlation can be identified by looking at the correlation between ΔV_k which is known from conventional meters.

Therefore, in order to establish the power quality monitor placement method, the following steps are followed:

1) Correlation of ΔV_k is obtained for all pairs of buses with the information from regular meters during a certain number of past weeks (typically, one week will be used in this work). A matrix $\mathbf{C}$ with correlation between every bus (like the one in the left of Fig. 2) is built.
2) Location of monitored buses will be chosen so that any non-monitored bus must have high correlation with a monitored one.
   To this aim, the following optimization process is followed:
   a) A correlation threshold value δ is chosen in order to consider the minimum correlation required between monitored and non-monitored buses (typically, this correlation threshold will be a value around 0.9, but the influence of this parameter will be further discussed in Section VII).
   b) A new binary correlation matrix $\mathbf{C_{bin}}$ is built from $\mathbf{C}$. A generic element $c_{bin}(i,j)$ of $\mathbf{C_{bin}}$ is obtained by means of the following expression:

$$c_{bin}(i,j) = \begin{cases} 1, \text{ if } c(i,j) \geq \delta \\ 0, \text{ otherwise} \end{cases} \tag{2}$$

   where $c_{bin}(i,j)$ and $c(i,j)$ are the element i,j of matrices $\mathbf{C_{bin}}$ and $\mathbf{C}$ respectively.
   If the element $c_{bin}(i,j)$ is equal to 1, it means that buses i and j are highly correlated.
   c) A binary array $\boldsymbol{y}$ is defined for the placement of power quality monitors. This array has N_b elements, where N_b is the total number of buses in the system. If a generic element i of $\boldsymbol{y}$ is $y(i) = 0$, it means that there is not a monitor in bus i, whereas $y(i) = 1$ means that a power quality monitor is installed in i.
   The minimum number of meters that allows monitoring the whole network has to be found. This means that the objective function of this optimization problem is:

$$\min_y \sum_{i=1}^{N_b} y(i) \tag{3}$$

   d) In order to guarantee that any bus in the network is within the observability area of a monitor, a high correlation between a non-monitored bus and any monitored bus is needed. Relating this statement to previously defined matrices, this implies that element $c_{bin}(i,j)$ must be equal to 1 for any generic non-monitored bus i and at least one monitored bus j. Therefore, the product of any row i of matrix $\mathbf{C_{bin}}$ multiplied by the array $\boldsymbol{y}$ should be greater than 1, meaning that there is at least one monitored bus j with high correlation to bus i. This can be mathematically expressed in the form of the following optimization problem:

$$\min_y \sum_{i=1}^{N_b} y(i) \text{ subject to} \begin{cases} y(i) = \{0,1\} \\ \mathbf{C_{bin}} \cdot \boldsymbol{y} \geq \{1,1,\ldots,1\}^T \end{cases} \tag{4}$$

   The solution of this minimization problem assures that there is a correlation higher than the selected threshold δ between every non-monitored bus and a monitored one. When a bus is highly correlated to more than one monitored bus, it is assigned to the bus with the highest correlation.

If some PQ monitors are already installed in the network or their location is decided by any other criterion, they can be integrated in this approach by forcing the optimization problem to place a monitor in a specific bus, i.e., forcing $y(i) = 1$ at that bus i.

It is important to note that the procedure to locate PQ monitors is performed just once, while the estimation algorithm is performed on a continuous basis for continuous distortion

estimation. The estimation methodology that will be described in Section IV relies on this decision of PQ monitoring.

IV. Method for Harmonic Estimation

Once the location of PQ monitors is decided in the RDN, harmonic voltages can be estimated at non-monitored buses. It is important to bear in mind that one of the difficulties of this step is that network parameters and topology are assumed unknown in this method. The estimation methodology consists on two steps:

a) Modeling of harmonic current injections: the harmonic current injections of all the system buses are modeled.
b) Algorithm for harmonic voltages calculation: the estimated harmonic current injections from each residence are used to calculate harmonic voltages in the whole network.

These two steps are explained in the two following subsections.

PQ monitors installed according to the methodology explained in Section III are capable of recording harmonic voltages and harmonic currents at the point of connection of residential customer (mainly single-phase). Examples of low-cost PQ analyzers can be found in [25]–[28].

Note that, in the developed methodology, buses without PQ monitor are supposed to be equipped with a conventional smart meter, as it is common in European residential distribution systems [23]. The averaging time resolution for both, PQ meters and smart meters, will determine the time resolution for the estimation of harmonic distortion at non-monitored buses. In the tests conducted in this work, 10-minutes resolution has been selected.

A. Modeling of Harmonic Current Injections

Harmonic currents are directly known at buses with a PQ monitor installed. This information is used to build a model of harmonic injections which will be applied to estimate the injected harmonic currents in the rest of non-monitored buses.

Some previous approaches have been based on obtaining statistical distributions of injected harmonics from data gathered in measurement campaigns performed in a specific moment in the past [12], [13], [29]. These statistical distributions were afterwards sampled to simulate harmonic currents that ideally match the real ones. This approach has been improved in two different ways in this work. First, instead of basing the injection models on past measurement campaigns, continuous information collected from PQ monitored buses is used to extract typical distributions of injections for the whole network. This assures a continuous updating of demand conditions. Otherwise, if demand conditions change (e.g., because of the inclusion of new types of loads, such as LED lighting in the past 10 years [30]), models obtained from past measurements can lack representativity. The same can happen if measurements were performed under some specific conditions that do not represent the complete variability of the scenarios (e.g., harmonic injection measured during the winter is not the same as harmonic injection during the summer [13], [31]).

In addition, in this work, kernel non-parametric (kNP) distributions [32] are used to model harmonic current injections at network buses. Kernel density estimation is a non-parametric method to estimate probability distributions. A kNP distribution can be interpreted as a mixture of Gaussian distributions that fits the data accurately and smooths any type of complicated histogram [32]. For fitting to a specific kNP, in this work, MATLAB Statistics and Machine Learning Toolbox is used [33]. While typical parametric statistical distributions (such as normal, log-normal, etc.) are simple to use and characterize, very often do not include the variety and complexity of data that multiple order harmonic injections have and, consequently, they can have some inaccuracies fitting the real data. One advantage of non-parametric functions is that they can be adjusted much more precisely to the real distribution of data. All kNP calculated in this work use normal smoothing function and a theoretical optimal bandwidth, computed automatically by MATLAB Statistic and Machine Learning Toolbox [33].

Thus, harmonic currents measured continuously during one week with the data provided by PQ meters at monitored buses are used to obtain the parameters of kNP distributions. These kNP distributions are then used to estimate harmonic currents of the ongoing week at non-monitored buses.

For obtaining kNP distributions, demand is segmented into different per-unit powers and each current magnitude is modeled piecewisely [13]. By doing this, harmonic currents can be modeled in % without misleading the influence of fundamental current demand.

For modeling phases, a similar methodology is followed, but segmentation is done in harmonic magnitudes. To explain the variability of harmonic phases, different intervals of demanded power could be used, as it was done to characterize harmonic magnitudes. However, to better understand which variable better explains the variability of phases, a principal component analysis [32] has been conducted. The principal component analysis concluded that the variability of arguments is better explained by magnitudes (second contributor to principal components obtained in the analysis, with variance of 2119) than by demanded power (the least important variable, with variance of 0.06). With this, it can be concluded that segmenting phases data in demanded power intervals is less representative than segmenting according to magnitude intervals.

An example of kNP modeling is shown in Figs. 3(c) and 4(c). Fig. 3(c) shows the probability distribution function (PDF) of current magnitudes for 3^{rd} and 5^{th} harmonics measured in 20 different dwellings in Madrid, Spain, during one week (in blue) and the obtained kNP distribution (in red) for different intervals of demanded power (P).

Fig. 4(c) presents the kNP distribution for 3^{rd} and 5^{th} harmonic current phases for the same measured dwellings. In this case, as in phase modeling, segmentation is done for different intervals of current magnitudes. Fig. 4(c) shows the probability distribution function of the actual phases measured during a week in 10-minute interval at customer permises and its kNP distribution (in red).

Therefore, in the proposed method the following steps are followed for estimation of harmonic currents injection:

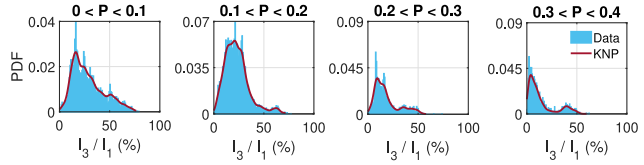

(a) 3rd current magnitude.

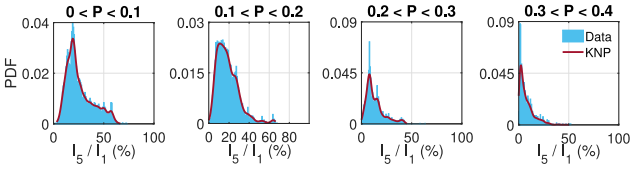

(b) 5th current magnitude.

Fig. 3. Probability distribution function for harmonic magnitudes segmented in demanded power intervals (blue) and its kNP distribution (red).

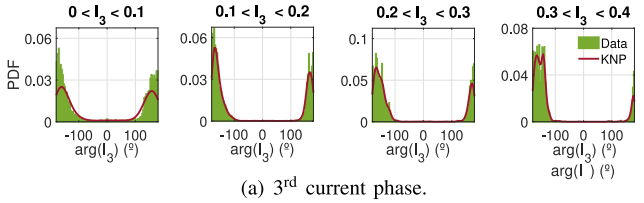

(a) 3rd current phase.

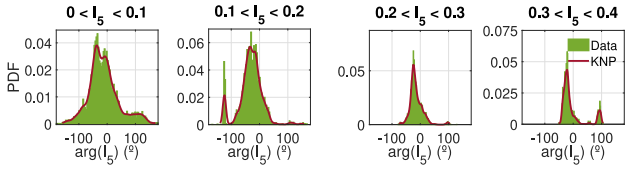

(b) 5th current phase.

Fig. 4. Probability distribution function for harmonic phases segmented in current magnitude intervals (green) and its kNP distribution (red).

1) Non-parametric probability distributions are obtained for harmonic magnitudes and phases with the real data monitored at PQ monitors. These distributions are segmented by power values (magnitudes) and by magnitude values (phases).
2) The harmonic injection of each residence is obtained by sampling the non-parametric probability distribution (according to the measured demand on each bus) calculated for each harmonic order.

B. Algorithm for Harmonic Voltages Calculation

In the previous step, harmonic injections from each residence were estimated by means of the obtained kNP distributions. With the estimated harmonic current injections, harmonic voltages at non-monitored buses must be estimated. The difficulty to do this estimation lies in the fact that the network parameters are assumed unknown as it is usual in practice in LV networks.

To overcome this lack of network data, a mathematical algorithm is proposed in this work which relates current injections to voltage harmonics. This algorithm, although based on simplifying hypothesis, has proved to provide good results as it will be shown later. This mathematical algorithm can be understood in a more intuitive way through the electrical

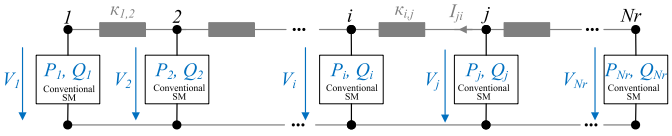

Fig. 5. Radial equivalent electric circuit.

equivalent circuit shown in Fig. 5. However, it is important to bear in mind that this equivalent circuit does not pretend to be and exact representation of the real physical elements and topology of the network, but to work as an equivalent that allows representing the mathematical equations obtained and the relation among variables throughout an electrical simplified representation.

In the first stage of the process (Section III) PQ monitors were located so that any other bus of the network has a high ΔV_k correlation with one monitored bus. Therefore, each monitored bus has a high correlation area made up of buses that have high ΔV_k with it. The process that will be described hereafter is applied to each group of buses made up of a monitor and the buses inside its monitoring area. Fig. 5 represents the group of buses inside the correlation area of a certain monitor. As stated above, this circuit is not intended as a real representation of the network configuration, but as a model. Each of the buses in the group is equipped with a conventional smart meter that provides the value of fundamental voltage, as well as active and reactive power (the possibility of non-available reactive power is also studied in Section VI-D). Therefore, these magnitudes are collected at each bus. Buses are numbered according to their value of fundamental voltage magnitude, so that bus number 1 will be the bus with the highest value of fundamental voltage and bus N_r will be the bus with the lowest fundamental voltage in the group, where N_r is the number of buses in the monitor group. That is, $V_i > V_j$ with $i < j$, where i and j are two generic buses inside the same correlation group. Buses in the group are sorted by the same descending order in the radial equivalent.

All the buses in the group ordered in this way will be assumed to be electrically connected in an "equivalent radial connection" by means of coefficients $\kappa_{i,j}$ with impedance dimensions. Assuming this type of equivalent, voltage at each pair of buses (which are known by measurements), can be related with the following expression:

$$\kappa_{i,j} \simeq \frac{V_j - V_i}{I_{ji}} \tag{5}$$

where V_i represents the voltage at a generic bus i, V_j represents voltage magnitude at a generic bus j with $i < j$, and current I_{ji} is the total current injected from bus j to bus i.

Expression (5) is approximate since just voltage magnitudes are used for the calculation instead of complex values, because fundamental voltages V_i and V_j at different buses in the network have a small phase difference, usually below 5° or 0.1 *rad* [15]. Voltages V_i and V_j in the numerator of (5) are directly obtained from conventional monitors installed at each residence. Current in the denominator of (5) can be approximated by the sum of the active and reactive power demanded by all loads connected to the right side of bus j, i.e., by

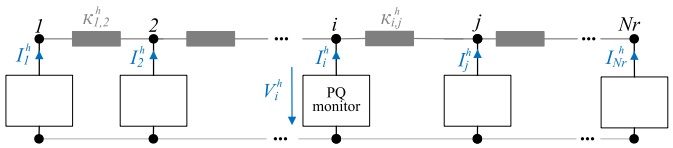

Fig. 6. Radial equivalent electric circuit for harmonic frequencies.

any generic bus k with $k \geq j$. This can be mathematically expressed by:

$$\kappa_{i,j} \simeq \frac{V_j - V_i}{\sqrt{\sum_{k=j}^{Nr}(P_k^2+Q_k^2)}/V_j} \tag{6}$$

where P_k and Q_k represent the active and reactive power demand at any generic bus k.

Equation (6) allows calculating parameter $\kappa_{i,j}$ for each pair of buses from values that are known from measurements performed by means of the conventional smart monitors installed at each bus. Note that the parameter $\kappa_{i,j}$ has impedance units (Ω) and that in (6) active and reactive losses are neglected since just loads consumption is considered.

The mathematical model obtained for fundamental magnitudes can be extended now to harmonic orders by extending the relations previously obtained to harmonic frequencies as shown in Fig. 6 where:

- Voltage harmonic is known just at one bus of the group, which is the bus equipped with a PQ monitor (the monitored bus is considered bus i in the figure).
- Harmonic current injection is measured at the PQ monitored bus, bus i, and it has been estimated at the rest of the buses as discussed in Section IV-A.
- Parameter $\kappa_{i,j}$ which expressed the relation between variables for fundamental magnitudes according to (6), has to be corrected for harmonic frequencies. For a certain harmonic order h, the corrected coefficient $\underline{\kappa}_{i,j}^h$ can be expressed as:

$$\underline{\kappa}_{i,j}^h = \kappa_{i,j}(r + jh \cdot x) \tag{7}$$

where r and x are factors to transform $\kappa_{i,j}$ into a complex number preserving its magnitude so that:

$$\sqrt{r^2 + x^2} = 1 \tag{8}$$

The ratio r/x is a value typically comprised between 5 and 10 which is similar to the R/X ratio of lines in European RDNs [34], [35]. Its value and the dependency of r with frequency will be further discussed in Section VII-B.

Harmonic voltages at a generic bus j adjacent to bus i (with the PQ monitor) are calculated as follows:

$$\underline{V}_j^h = \underline{V}_i^h + \underline{\kappa}_{i,j}^h \sum_{k=j}^{N_r} \underline{I}_k^h \tag{9}$$

where $\underline{V}_i^h$ has been obtained from the PQ meter, $\underline{\kappa}_{i,j}^h$ is obtained from (7) and (8), and $\underline{I}_k^h$ are estimated as explained in Section IV-A. In this way, by applying (9) repeatedly to different buses, harmonic voltages can be estimated in a straightforward way for all system buses.

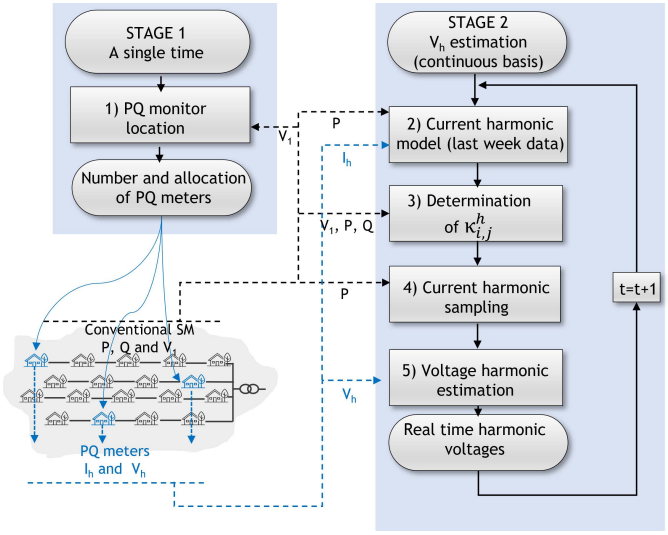

Fig. 7. Flowchart of the methodology.

This process is applied with the time resolution provided by the monitors. Ideally, if monitors provide sufficient time resolution, the methodology should be applied every 10 minutes, in order to compare to PQ standard EN50160 [36]. Equations (6) and (9) are very simple equations that allow a very fast computation time which permits the calculation of harmonic voltages at non-monitored buses in a very efficient way and practically in real time.

Results, examples and method accuracy are shown and discussed in next sections.

C. Discussions on the Practical Application of the Method for DSO

After explaining each of the stages of the methodology, this section summarizes the overall process in a practical way in a process that is illustrated in Fig. 7.

1) PQ monitor location is decided based on the voltage magnitudes registered during a week by conventional SM. This process is performed just once.
2) Harmonic currents are monitored during a week at buses equipped with a PQ monitor. With this measurements, statistical distributions are obtained that will be applied to determine injections at non-monitored buses.
3) Determination of parameters $\underline{\kappa}_{i,j}^h$ with (6) and (7), with real time data from the convention SM.
4) Sampling of current injection distributions of step 2) according to the power demanded by the load and registered in the SM.
5) Equation (9) is applied to obtain voltage harmonics at each time step.

This methodology has been developed to be applied in LV residential networks, which usually have radial or almost radial topologies.

Its application depends on the deployment of PQ meters in a small number of buses, whereas all customers are supposed to have a smart meter installed. All customers connected to the network are supposed to be residential, with similar demand patterns.

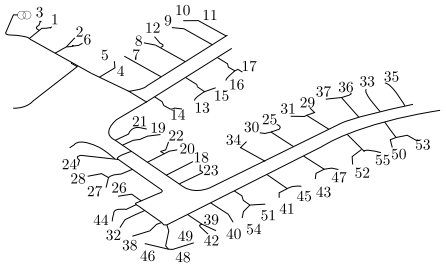

(a) IEEE LV European feeder.

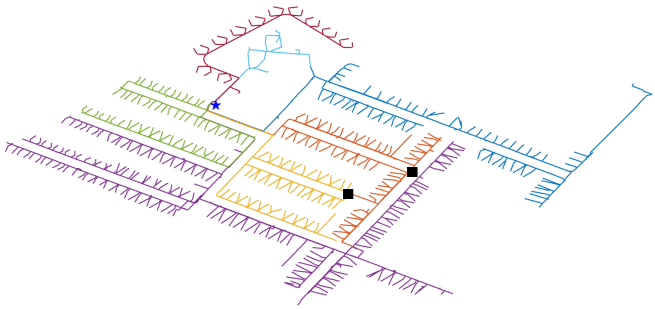

(b) LVN test network #7.

Fig. 8. One-line diagrams of test feeders used for validation.

V. Strategy for Validation of the Estimation Method

This section presents the strategy and assumptions followed to validate the proposed methodology. The considered test networks and the procedure to synthetically obtain pseudo-measurements that account for the stochastic nature of injections are also described.

A. Test Networks

To validate the proposed methodology, two different LV residential networks have been used, one of them being small, and the other medium-large. Both of them are realistic networks representing residential distribution feeder architecture and characteristics for Europe. They are based on published models [24], [37], so that results can be replicated.

The first one is the IEEE LV European test feeder [24]. This is a RDN with 55 residential single-phase customers connected to the LV side of a 11/0.4 kV transformer. The one-line diagram of the network is shown in Fig. 8.

The second case study corresponds to a more realistic and larger size network, the LVN test network #7 [37]. This network is composed of 471 residential customers connected to the LV side of a 11/0.4 kV transformer through 7 different feeders, and is shown in Fig. 8(b). In the single-line diagram, black squares represent switches, that are originally opened in the network.

B. Simulation of Harmonic Pseudo-Measurement

In order to test the performance of the proposed method in different scenarios and under a wide range of conditions, in this work, harmonics injected by residences have been synthetically simulated using a probabilistic approach that accounts for the stochastic nature of the phenomenon.

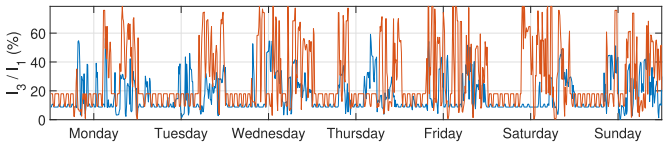

Fig. 9. Example for pseudo-measured 3rd harmonic currents at two random residences

Current injections of residences have been generated following a bottom-up approach, by combining the demand model developed by CREST [38] and the measured harmonic spectrum of household loads available in PANDA database [39] including associated uncertainties and stochastic behavior. These synthetically generated current harmonics will be used for validation purposes.

As a first step in the process of pseudo-measurement simulation, the number and type of appliances in each residence and their ON-OFF operation are simulated using the probabilistic demand models included in [40]. Once the operation state of the loads is probabilistically estimated considering their high stochastic nature, the magnitude and phase angle of harmonic currents injected during the ON state are synthetically generated. Their values are obtained by sampling characteristic multivariate Gaussian distributions which have been previously obtained for each type of residential appliance by performing cluster analysis techniques [32] to the set of harmonic currents measured in PANDA database [39]. In this way, the variability in the harmonic injection among different devices of a certain type of appliance is incorporated in the model. For devices with very little data available in PANDA, additional measurements have been performed.

This bottom-up approach allows obtaining the total harmonic current injection of each residential consumer connected to the network.

An example of weekly pseudo-measured 3rd harmonic current is showed in Fig. 9 for two random residential consumers. Day and night periods can be differentiated from the figure, but the time evolution is highly random.

These synthetically generated currents are considered as the real currents injected in the test network. By using these currents, fundamental and harmonic voltages at each bus are obtained from simulation with OpenDSS using a conventional power flow and a harmonic load flow. Loads are modeled as constant P and Q loads at fundamental frequency and as Norton equivalents at harmonic frequencies [41].

Voltage values calculated in this way are used as real values in order to compare with the harmonic voltages estimated by means of the proposed method, and to assess its accuracy.

In the estimation process, just the values that would be measured are assumed to be data of the estimation method, i.e., fundamental voltage magnitude, active power and reactive power at all consumer buses and current and voltage harmonics at a reduced number of buses equipped with PQ monitors.

Network parameters and topology are not used in the process to estimate harmonic voltages in the proposed methodology.

C. Validation Assumptions

The following conditions have been used for the calculation of the results presented in the following sections:

- In the IEEE LV European test feeder [24] 3 PQ meters are considered, while in the LVN #7 [37] 48 PQ meters were assumed to be connected. The location and area of correlation of these monitors will be further discussed in Section VI-A.
- In the estimation method, the probability distribution of harmonic current injections of each consumer is estimated with the measurements registered by PQ monitors during the previous week.
- A ratio $r/x = 5$ is used for the parameters shown in (8).
- In the primary side of the main transformer, a background voltage distortion is assumed for the 5th and 7th harmonic voltages as reported in [42]. This background distortion is assumed to make simulations more realistic, but the main source of harmonic distortion in LV busbars is harmonic injections and not background distortion coming from MV side [43].
- The analysis performed has studied odd harmonic order up to 17th order. A time step of 10-minute has been used for calculations and the estimation has been performed during a period of one week.

VI. Validation Results

This section shows the result obtained using proposed method in different case studies, i.e., those used for the validation.

A. Analysis of Stage 1: PQ Monitor Location

The method for PQ location was described in Section III. According to this method, PQ monitors must be located so that each bus of the network non-equipped with a PQ meter must be inside the area with high ΔV_k correlation with one of the monitored buses. The application of this monitor location criterion to the IEEE LV European test feeder leads to placing 3 PQ monitors at buses 5, 8, and 38 when 0.9 is set as the correlation threshold.

Fig. 10(a) shows the ΔV_k correlation matrix already depicted in Fig. 2 for all the buses. This matrix would be built with the fundamental voltages measured at all system buses during one week using conventional smart meters. On the right, in Fig. 10(b), columns corresponding to the three monitored buses are extracted from the whole matrix, i.e., columns 5, 8, and 38, which are shown slightly enlarged. By looking at all the rows in these two columns, it can be seen that any bus of the network (associated to a row) has a high correlation at least with one of the three monitored buses corresponding to one of the three columns.

A similar result is shown for the LVN test network #7. In this case, 48 PQ meters are installed and a 0.93 correlation threshold is applied to associate the non-monitored buses with the monitored ones. In a similar way to Fig. 10, Fig. 11(a) shows the correlation matrix for the whole network (471 buses). In the middle, Fig. 11(b), shows (with a small enlargement for a better view) just the columns corresponding

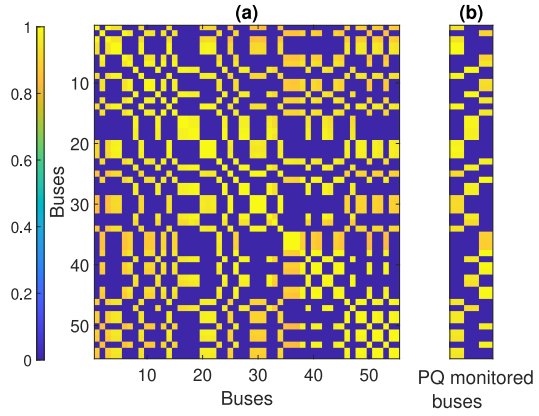

Fig. 10. ΔV_k correlation matrices for all the buses (a) and for PQ monitored buses (b) in the IEEE LV European test feeder.

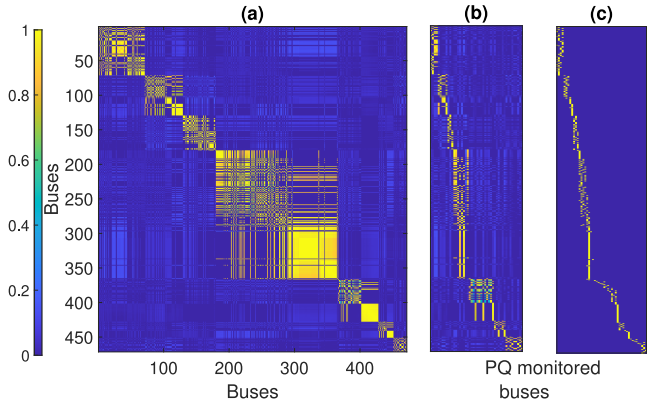

Fig. 11. ΔV_k correlation matrices for all the buses (a), for PQ monitored buses (b), and correlation area of monitors (c) in the LVN test network #7.

exclusively to the 48 monitored buses. In this case, it can be seen that some rows (corresponding to certain buses of the network) are highly correlated with more than a monitored bus. In such cases, non-monitored buses are allocated to the area of the monitored bus with the highest correlation with the non-monitored one. Finally, in Fig. 11(c), on the right, the final correlation area of each monitored bus (represented by a column) is shown by applying the aforementioned criterion. Therefore, in Fig. 11(c), for each row, a single column is highlighted indicating to which monitor's correlation area the bus is allocated.

B. Analysis of Estimation of Current Harmonic Injections

As explained in Section IV-B, the second stage of the method requires modeling the harmonic current injection of each residence in order to estimate voltages harmonics at all system buses. This modeling was performed by using non-parametric distribution functions from values recorded at the limited number of meters.

The performance of this step is analyzed here for the LVN test network #7. In Fig. 12, the probability distribution function of harmonic current magnitudes injected by the 471 residences of the network during a week is shown for 3rd, 5th and 7th harmonic orders. Colored in blue, the synthetically-generated distribution of currents injected during a week is shown. This

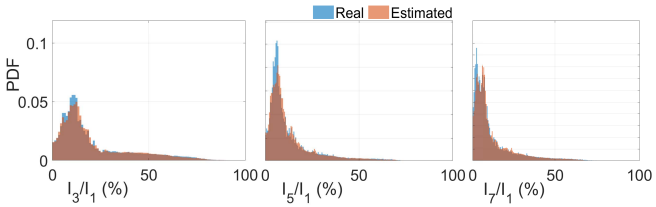

Fig. 12. PDF of real and estimated magnitude of harmonic current injections.

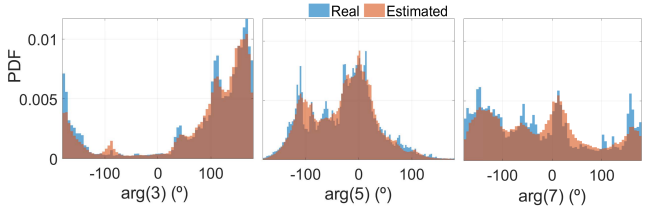

Fig. 13. PDF of real and estimated phase of harmonic current injections.

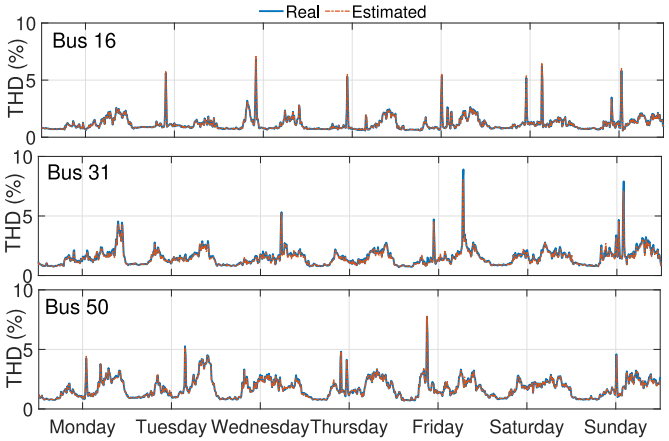

Fig. 14. Voltage THD during one week for three different buses (13, 31, and 50) of IEEE LV test feeder.

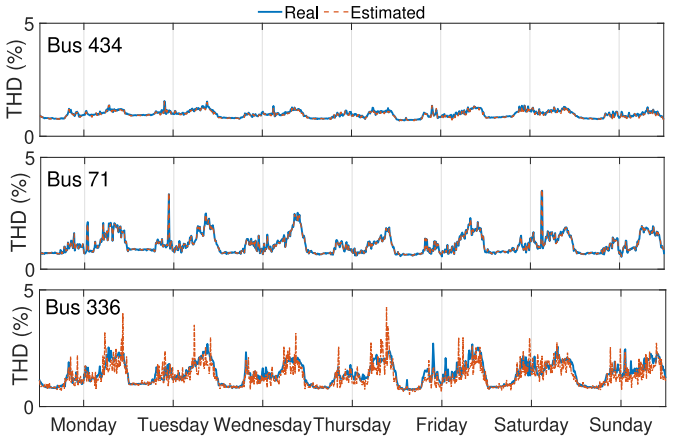

Fig. 15. Voltage THD during one week for three different buses (71, 336, and 434) of LVN #7 test feeder.

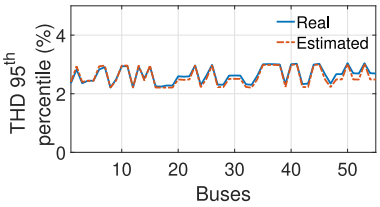

(a) IEEE LV European test feeder.

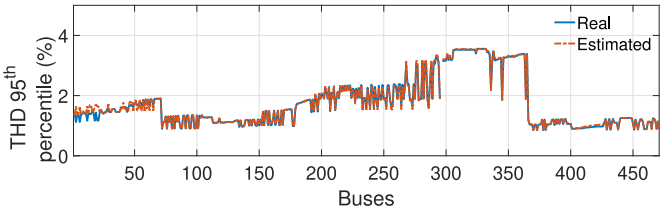

(b) LVN #7 test feeder.

Fig. 16. Weekly 95th voltage THD percentile for network buses.

distribution, referred as *real* in Fig. 12, would be unknown in a field application. Colored in orange, the distribution obtained for the same week with the proposed estimation method is shown. It can be seen that the proposed estimation method (based on randomly sampling kNP distributions modeled with the data registered by PQ monitors during the previous week) provides a highly similar distribution of harmonic magnitudes.

Fig. 13 shows a similar comparison of probability distribution functions but, in this case, refers to the phase angles of 3rd, 5th and 7th harmonic currents. Again, a good performance of the estimation method is observed.

C. Performance of the Harmonic Estimation Method

Previous sections showed partial results of the method in order to provide a better understanding of the performance of different steps. In this section, the accuracy of the complete methodology is assessed. The test networks used are described in Section V-A and the validation conditions were explained in Section V-C.

In Fig. 14, the evolution of THD values during one week is shown for three randomly chosen non-monitored buses of the IEEE LV European test feeder. A similar result is shown in Fig. 15 for three non-monitored buses of the LVN #7 network. In both networks, it can be observed a very variable evolution of THD values along the week at different buses. However, a good fitting is observed in all the cases between the real THD experienced at the non-monitored buses and the THD estimated by the method. THD is calculated here with 10-minute time resolution. Therefore, 1008 THD values are estimated in each week for each bus. The 95th percentile of these values is subjected to limits compliance in accordance with standard [36]. Hence, the estimation of the 95th percentile at each bus can be of interest in order to compare with standard limits.

Fig. 16 presents the real and estimated 95th THD percentile in a week for all the buses at the IEEE LV European test feeder. Fig. 16(b) shows a similar result for the larger 471-bus network. In both networks, a good performance of the estimation method is achieved for the estimation of the 95th THD percentile, with a mean estimation error of 0.04% and 0.027% for the IEEE LV European test feeder and for the 471-bus network, respectively. The maximum

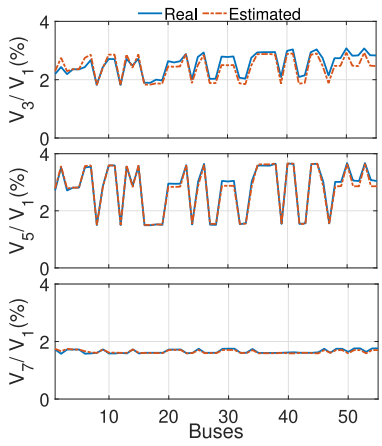

(a) IEEE LV European test feeder.

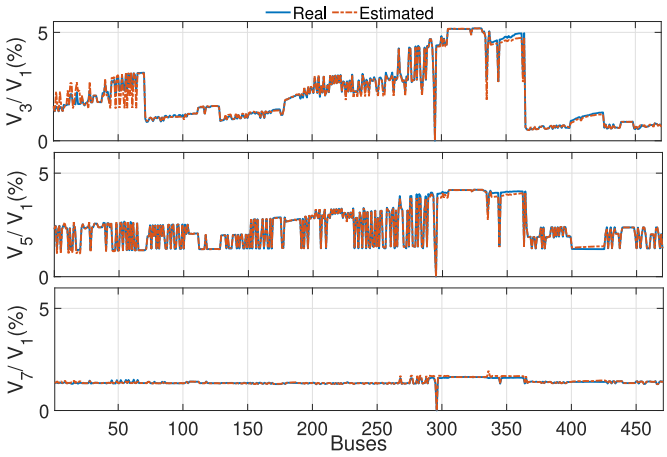

(b) LVN #7 test feeder.

Fig. 17. Weekly 95th percentile for different voltage harmonic orders at all system buses.

absolute estimation errors in these two networks were 1.17% and 2.14%.

The proposed estimation method has also been checked for the estimation of individual voltage harmonics. Figs. 17 and 17(b) show the real and estimated 95th percentile of harmonic voltages of orders 3, 5 and 7 at all the buses at the IEEE LV European test feeder and at the LVN #7 network, respectively. These values can be compared with standard limits to assess standard compliance and, as it can be observed in Figs. 17 and 17(b), a good performance of the estimation method is also observed for the estimation of individual harmonic voltages. For instance, the average and the maximum absolute error of estimation of 3rd harmonic in the IEEE LV European test feeder are 0.09% and 1.22%, respectively, and 0.05% and 2.62% in the 471-bus network.

D. Estimation of Reactive Power Demand

It is common that smart meters installed in residential customer's point of common coupling record voltage and energy consumed in a certain time interval [44]. From these values, mean demanded active power can be easily obtained.

In some cases, reactive power demand, needed in this work in (6), could be an unknown data due to smart meter

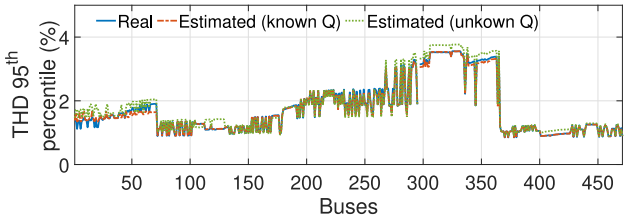

Fig. 18. Weekly 95th voltage THD percentile for network buses of the LVN #7 network with known and estimated reactive power.

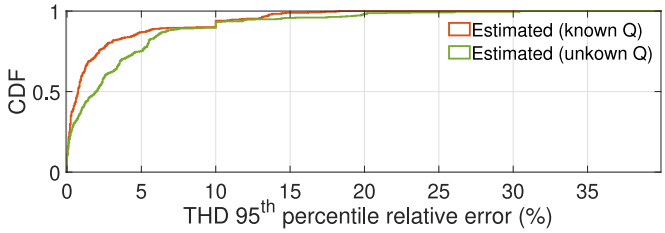

Fig. 19. CDF of relative error in the estimation of 95th THD percentile with known and estimated reactive power at buses of the LVN #7 network.

limitations. If this is the case, this section proposes a methodology to estimate their values. This methodology is based on a similar technique as the one followed to estimate harmonic currents at non-monitored buses in Section IV-A.

The methodology proposed consists of:

1) Reactive power is registered during one week at the buses with an installed PQ monitor.
2) Registered reactive power consumption is segmented in different intervals according to the value of active power demand at the same time interval, as it was proposed for segmenting measured harmonic currents.
3) A kernel non-parametric distribution of reactive power values is built for each considered active power interval.
4) In order to apply (6) when estimating real-time harmonic voltages, the reactive power demanded at a certain bus is estimated by randomly picking a sample of the kernel non-parametric distribution corresponding to the interval with the active power demanded at a that bus.

The utilization of estimated reactive powers leads to an increase of the error of the overall estimation at certain buses, but, as it is shown in Fig. 18 (weekly 95th percentile of THD) and Fig. 19 (CDF of relative error in estimating 95th percentile of THD), the performance of the methodology is still accurate. This figure compares the case study presented in Section VI-C, and the same case study where reactive power is unknown.

VII. Discussion on Accuracy and Robustness

Several variables of the proposed method can influence its performance. In this section, the values adopted in this work are discussed and their influence on the accuracy of the method is assessed.

A. Number of Monitors

Number of PQ monitors installed is a key aspect in the application of the methodology. The decision on this

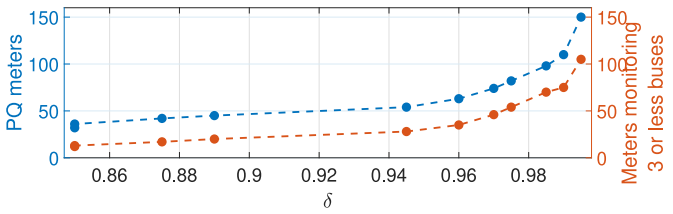

Fig. 20. ΔV_k correlation threshold (δ) and number of monitors.

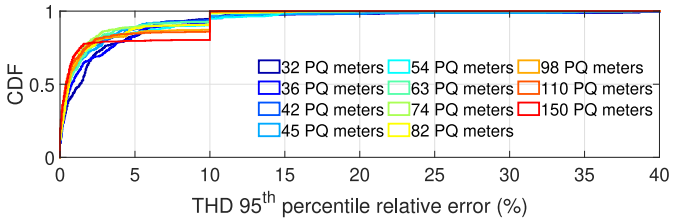

Fig. 21. CDF of relative error on estimating THD 95$^{\text{th}}$ percentile for different number of monitors.

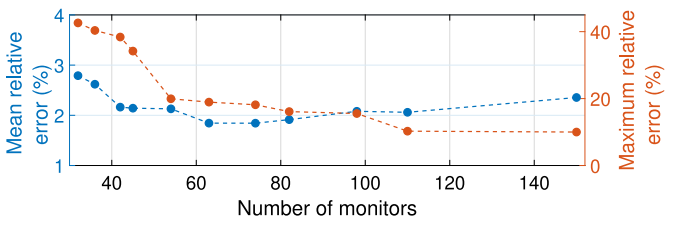

Fig. 22. Mean and maximum relative error on estimating THD 95$^{\text{th}}$ percentile with different number of monitors.

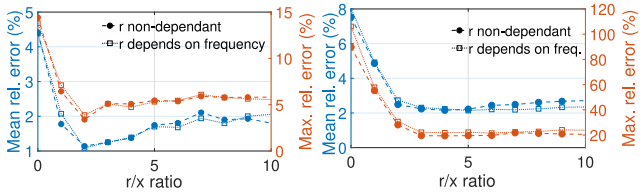

(a) IEEE LV European test feeder. (b) LVN #7 network.

Fig. 23. Mean and maximum relative error in estimating THD 95$^{\text{th}}$ percentile with different r/x ratio and model of dependency of r with frequency.

number depends on economical constraints (number of PQ meters available to install by the DSO), and on the desired performance of the method, since accuracy is influenced by the PQ meter deployment.

To illustrate this idea, several simulations have been run in the LVN #7. PQ monitors have been placed according to the strategy described in Section VI-A but, in this case, the number of monitors has been modified by modifying the correlation threshold required to define the correlation area of a PQ monitor. To illustrate this fact, Fig. 20 compares the number of monitors (in the left axis) obtained for different δ. Fig. 20, referring to the right axis, also plots the number of PQ meters that monitor only three or less buses. It can be observed that when the number of monitors increases, there are more monitors that cover only a small number of buses. This means that, while the cost of monitoring increases, the increase of accuracy affects a small area of the network around each new monitor.

In order to assess the influence of the number of monitors on accuracy, Fig. 21 shows the cumulative distribution function (CDF) of relative errors in estimating THD 95$^{\text{th}}$ percentile at non-monitored buses. For small numbers of monitors deployed in the network, THD 95$^{\text{th}}$ errors are greater; whereas higher penetration of PQ monitors leads to smaller errors in most of the buses.

To provide a simple metric that can help to decide how many PQ meters need to be installed, depending on the desired accuracy of the methodology, Fig. 22 presents the mean and maximum relative errors in estimation of THD 95$^{\text{th}}$ percentile with different number of PQ meters. Connecting the PQ monitors to over 10% of the network buses produces a very slight decrease in errors. The error remains at about 2% once the number of monitored buses is 10% or more.

B. Ratio r/x and Dependency of r With Frequency

In Section IV it was stated that) a ratio r/x between 5 and 10 was adequate in (7), based on past experience [34], [35]. The case studies presented in Section VI were run considering a ratio $r/x = 5$ in the estimation algorithm. Different values of this parameter have been applied for both IEEE LV European test feeder and LVN #7 network and the accuracy of the method has been assessed. The dependency of r with the frequency has also been explored by considering the model [45] expressed as:

$$\underline{\kappa}^{h}_{i,j} = \kappa_{i,j}\left[r \cdot (0.187 + 0.582 \cdot \sqrt{h}) + jh \cdot x\right] \tag{10}$$

Fig. 23(c) shows the mean relative error (in the left vertical axis) and maximum relative error (right vertical axis) in the estimations of weekly 95$^{\text{th}}$ THD percentile in both tested networks and for the models defined in (7) and (10). It can be seen that the variation of this parameter between 5 and 10 does not have, if at all, a significant effect on the method accuracy. However, very low values (typically lower than 2) of this ratio lead to higher errors. Infinite r/x ratio has also been tested with no improvement on accuracy. Models given by (7) (neglecting the dependency of r with frequency), and model (10) (including this dependency) provide similar results.

C. Influence of the Period of the Year

Results shown in Section VI have been obtained for the power demand and harmonic injection of a random summer week. Demand and therefore, harmonic injections, are influenced by the period of the year (outside temperature, light hours, etc.). In order to justify the validity of the method for different weeks in different times of year, this section presents results for the harmonic estimation in four different weeks (each corresponding to a season: winter, spring, summer and fall) with the same number and location of PQ meters as proposed in Section VI.

Fig. 24 presents the CDF of relative error in the estimation of 95$^{\text{th}}$ percentile of THD at all the buses of the LVN #7 network for four different weeks, each of them in one season

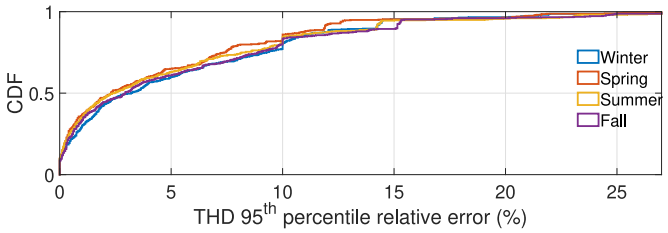

Fig. 24. CDF of relative error in the estimation of 95th THD percentile for different weeks in the year at buses of the LVN #7 network.

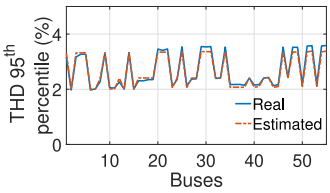

(a) IEEE LV European test feeder.

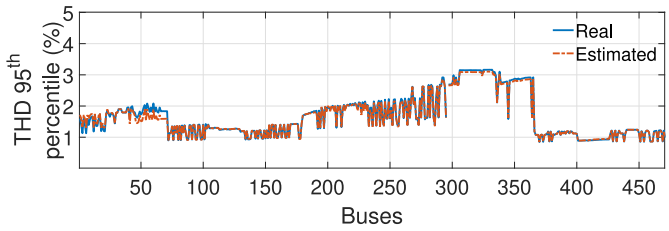

(b) LVN #7 test feeder.

Fig. 25. Weekly 95th voltage THD percentile for network buses in PV scenario.

of the year. Although results are different and show some variability due to the randomness of the values, similar accuracy is obtained in different weeks. Note that location of monitors is the same for all the tested weeks, as PQ monitors are installed in its location only once.

D. Influence of PV Generation

Today's residential network is subject to many changes, including the increasing spread of distributed generation, mainly PV.

In order to analyze if the presence of single-phase PV inverter interfaced devices jeopardizes the performance of the method, this case study is presented. This case study considers the same networks and assumptions described in Section VI-C, but 40% of residences are assumed to have PV distributed generation, as a high penetration scenario [46]. The same number and location of power quality monitors of Section VI-C has been considered in this case study.

Fig. 25(c) presents the real and estimated 95th THD percentile during one week for all the buses at the IEEE LV European (a) and the 471-bus network (b).

As it can be seen in Fig. 25(c), a very good performance of the method is achieved when the PV generation is widely deployed in the network, showing that the methodology is capable of estimating harmonic voltages in a grid with high penetration of inverter-based resources.

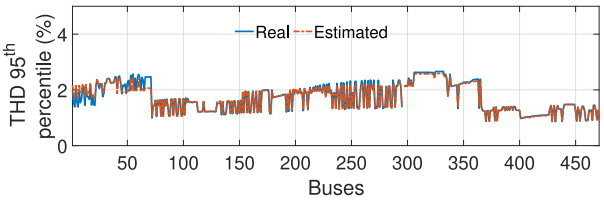

Fig. 26. Weekly 95th voltage THD percentile for network buses in case with closed switches.

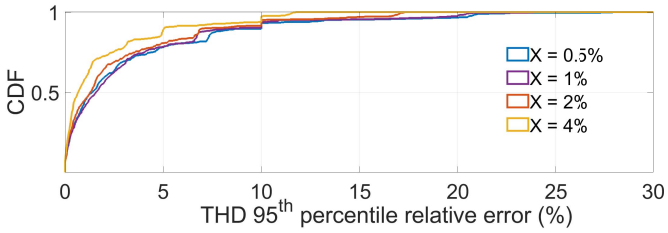

Fig. 27. CDF of relative error on estimating THD 95th percentile for different transformer leakage reactances (X) in LVN #7.

E. Network Topology

Two different networks with distinct radial configurations have been tested, and results, included in previous sections, showed comprising results. In this section, changes on topology in a network where PQ meters are already installed is studied. This case study focuses on analyzing the situation in which the estimation methodology is being used in a network, with installed PQ monitors, but some topology variations occur in the network (i.e., some switches change their position due to operational needs).

This situation is studied by applying the PQ monitor location explained in Section VI-A (48 monitors in LVN #7) and analyzing the performance of the estimation method when switches are closed. Switches are marked as black squares in Fig. 8(c), and are closed in this case study.

Fig. 26 shows the estimated and pseudo-measured THD 95th percentile at network buses. Results show a good performance, leading to a slight THD underestimation at some buses. In any case, estimations are still close to real THD values, with relative errors in estimating THD 95th percentile below 10% in 90% of the buses.

F. Transformer Leakage Reactance

The last proposed robustness analysis studies how different leakage reactance of the main substation transformer can interfere with the performance of the methodology. Leakage transformer reactance has been identified as one of the key parameters that determine the harmonic distortion in LV side of the network [47]. In this section different transformer reactances are assumed in LVN #7 test feeder, leading to different levels of harmonic distortion in the network. The performance of the method under these conditions has been assessed.

A comparison between the relative errors in estimating THD 95th percentile when main transformer presents different leakage reactances is included in Fig. 27. As it can be seen, similar results are achieved for all the cases, with a better performance

when the leakage reactance is larger, due to the higher values of harmonic distortion obtained, that tend to minimize relative errors.

VIII. Conclusion

This paper presents a new practical method to estimate harmonic voltages at all buses in a residential distribution system of unknown parameters and topology when only a partial PQ monitoring program is implemented.

The method gathers information from conventional smart meters and from a limited number of PQ monitors. It has been demonstrated that a good estimation of voltage harmonics can be achieved in real time at all system buses with only 10% or less of the buses equipped with PQ monitors. The location of this reduced number of monitors is established using an optimization algorithm proposed in this paper and based on voltage correlations.

The voltage harmonic estimation method proposed can be used to verify compliance with PQ standards and to identify current and future harmonic issues in the network. The robustness of the method and the effect of several parameters on accuracy (topology, transformer leakage reactance, PV generation) has been studied. The performance of the method with different number of available PQ meters has also been assessed, which can help DSO to decide what is the appropriate number of PQ monitors that should be installed in their network.

Finally, some future areas of research have been identified, such as applying the methodology to higher voltage level networks, to different types of clients rather than residential, and the implementation of the methodology in a real network.

References

[1] H. Sharma, M. Rylander, and D. Dorr, "Grid impacts due to increased penetration of newer harmonic sources," *IEEE Trans. Ind. Appl.*, vol. 52, no. 1, pp. 99–104, Jan./Feb. 2016.

[2] F. Zare, F. Blaabjerg, P. Davari, G. W. Chang, and J. Adabi, "IEEE access special section editorial: Power quality and harmonics issues of future and smart grids," *IEEE Access*, vol. 7, pp. 132803–132805, 2019.

[3] Y. Wang, J. Yong, Y. Sun, W. Xu, and D. Wong, "Characteristics of harmonic distortions in residential distribution systems," *IEEE Trans. Power Del.*, vol. 32, no. 3, pp. 1495–1504, Jun. 2017.

[4] J. Meyer, A.-M. Blanco, M. Domagk, and P. Schegner, "Assessment of prevailing harmonic current emission in public low-voltage networks," *IEEE Trans. Power Del.*, vol. 32, no. 2, pp. 962–970, Apr. 2017.

[5] P. Rodríguez-Pajarón, A. Hernández, and J. V. Milanović, "Probabilistic assessment of the impact of electric vehicles and nonlinear loads on power quality in residential networks," *Int. J. Electr. Power Energy Syst.*, vol. 129, Jul. 2021, Art. no. 106807.

[6] D. Kumar and F. Zare, "Harmonic analysis of grid connected power electronic systems in low voltage distribution networks," *IEEE J. Emerg. Sel. Topics Power Electron.*, vol. 4, no. 1, pp. 70–79, Mar. 2016.

[7] S. Pukhrem, M. Basu, and M. F. Conlon, "Probabilistic risk assessment of power quality variations and events under temporal and spatial characteristic of increased PV integration in low-voltage distribution networks," *IEEE Trans. Power Syst.*, vol. 33, no. 3, pp. 3246–3254, May 2018.

[8] M. Bollen *et al.*, "Consequences of smart grids for power quality: Overview of the results from CIGRE joint working group C4.24/CIRED," in *Proc. ISGT-Europe*, Sep. 2017, pp. 1–6.

[9] IEA (2020), "Tracking Lighting 2020," IEA, Paris, France, 2020. [Online]. Available: https://www.iea.org/reports/tracking-lighting-2020

[10] A. M. Jungreis and A. W. Kelley, "Adjustable speed drive for residential applications," *IEEE Trans. Ind. Appl.*, vol. 31, no. 6, pp. 1315–1322, Nov./Dec. 1995.

[11] W. Zhou, O. Ardakanian, H.-T. Zhang, and Y. Yuan, "Bayesian learning-based harmonic state estimation in distribution systems with smart meter and DPMU data," *IEEE Trans. Smart Grid*, vol. 11, no. 1, pp. 832–845, Jan. 2020.

[12] S. Abdelrahman and J. V. Milanović, "Practical approaches to assessment of harmonics along radial distribution feeders," *IEEE Trans. Power Del.*, vol. 34, no. 3, pp. 1184–1192, Jun. 2019.

[13] X. Xiao, Z. Li, Y. Wang, and Y. Zhou, "A practical approach to estimate harmonic distortions in residential distribution system," *IEEE Trans. Power Del.*, vol. 36, no. 3, pp. 1418–1427, Jun. 2021.

[14] K. Dehghanpour, Z. Wang, J. Wang, Y. Yuan, and F. Bu, "A survey on state estimation techniques and challenges in smart distribution systems," *IEEE Trans. Smart Grid*, vol. 10, no. 2, pp. 2312–2322, Mar. 2019.

[15] J. Zhang, Y. Wang, Y. Weng, and N. Zhang, "Topology identification and line parameter estimation for non-PMU distribution network: A numerical method," *IEEE Trans. Smart Grid*, vol. 11, no. 5, pp. 4440–4453, Sep. 2020.

[16] I. D. Melo, J. L. Pereira, P. F. Ribeiro, A. M. Variz, and B. C. Oliveira, "Harmonic state estimation for distribution systems based on optimization models considering daily load profiles," *Electr. Power Syst. Res.*, vol. 170, pp. 303–316, May 2019.

[17] A. Moradi, J. Yaghoobi, A. Alduraibi, F. Zare, D. Kumar, and R. Sharma, "Modelling and prediction of current harmonics generated by power converters in distribution networks," *IET Gener. Transm. Distrib.*, vol. 15, no. 15, pp. 2191–2202, 2021.

[18] A. Ketabi, M. R. Sheibani, and S. M. Nosratabadi, "Power quality meters placement using seeker optimization algorithm for harmonic state estimation," *Int. J. Electr. Power Energy Syst.*, vol. 43, no. 1, pp. 141–149, 2012. [Online]. Available: https://www.sciencedirect.com/science/article/pii/S0142061512001706

[19] C. F. M. Almeida and N. Kagan, "Harmonic state estimation through optimal monitoring systems," *IEEE Trans. Smart Grid*, vol. 4, no. 1, pp. 467–478, Mar. 2013.

[20] C. Rakpenthai, S. Uatrongjit, N. R. Watson, and S. Premrudeepreechacharn, "On harmonic state estimation of power system with uncertain network parameters," *IEEE Trans. Power Syst.*, vol. 28, no. 4, pp. 4829–4838, Nov. 2013.

[21] P. Rodríguez-Pajarón, A. H. Bayo, and J. V. Milanović, "Forecasting voltage harmonic distortion in residential distribution networks using smart meter data," *Int. J. Electr. Power Energy Syst.*, vol. 136, Mar. 2022, Art. no. 107653.

[22] "D3.4 Smart Meters Architecture and Data Model Analysis, NOBEL GRID Project." 2016. [Online]. Available: http://nobelgrid.eu/deliverables/

[23] F. Tounquet and C. Alaton, *Benchmarking Smart Metering Deployment in the EU-28*. Luxembourg City, Luxembourg: Eur. Comm. Publ. Office, 2020.

[24] "IEEE European Low Voltage Test Feeder." Distribution System Analysis Subcommitteee: Distribution Test Feeder Working Group. May 2015. [Online]. Available: http://sites.ieee.org/pes-testfeeders/resources/

[25] E. Viciana *et al.*, "OpenZmeter: An efficient low-cost energy smart meter and power quality analyzer," *Sustainability*, vol. 10, no. 11, p. 4038, 2018. [Online]. Available: https://www.mdpi.com/2071-1050/10/11/4038

[26] K. Koziy, B. Gou, and J. Aslakson, "A low-cost power-quality meter with series arc-fault detection capability for smart grid," *IEEE Trans. Power Del.*, vol. 28, no. 3, pp. 1584–1591, Jul. 2013.

[27] W. L. Rodrigues, Jr., F. A. Borges, A. F. da S. Veloso, R. D. A. L. Rabêlo, and J. J. Rodrigues, "Low voltage smart meter for monitoring of power quality disturbances applied in smart grid," *Measurement*, vol. 147, Dec. 2019, Art. no. 106890. [Online]. Available: https://www.sciencedirect.com/science/article/pii/S026322411930747X

[28] A. J. Christe, S. Negrashov, and P. M. Johnson, "Design, implementation, and evaluation of open power quality," *Energies*, vol. 13, no. 15, p. 4032, 2020. [Online]. Available: https://www.mdpi.com/1996-1073/13/15/4032

[29] M. T. Au and J. V. Milanović, "Establishing harmonic distortion level of distribution network based on stochastic aggregate harmonic load models," *IEEE Trans. Power Del.*, vol. 22, no. 2, pp. 1086–1092, Apr. 2007.

[30] S. Rönnberg and M. Bollen, "Power quality issues in the electric power system of the future," *Electricity J.*, vol. 29, no. 10, pp. 49–61, 2016. [Online]. Available: http://www.sciencedirect.com/science/article/pii/S1040619016302159

[31] P. Rodríguez-Pajarón, A. Hernández, and J. Milanović, "Probabilistic assessment of harmonics in a residential network," in *Proc. ICHQP*, Sep. 2020, pp. 1–5.

[32] T. Hastie, R. Tibshirani, and J. Friedman, *The Elements of Statistical Learning: Data Mining, Inference, and Prediction* (Springer Series in Statistics). Cham, Switzerland: Springer, 2009. [Online]. Available: https://hastie.su.domains/Papers/ESLII.pdf

[33] *Statistics and Machine Learning Toolbox ™ User's Guide*. Natick, MA, USA: MathWorks, Inc., Mar. 2020.

[34] R. G. Cespedes, "New method for the analysis of distribution networks," *IEEE Trans. Power Del.*, vol. 5, no. 1, pp. 391–396, Jan. 1990.

[35] M. Nijhuis, M. Gibescu, and S. Cobben, "Gaussian mixture based probabilistic load flow for LV-network planning," *IEEE Trans. Power Syst.*, vol. 32, no. 4, pp. 2878–2886, Jul. 2017.

[36] *Voltage Characteristics of Electricity Supplied by Public Distribution Networks*, CENELEC Standard EN 50160, 2010.

[37] V. Rigoni, L. F. Ochoa, G. Chicco, A. Navarro-Espinosa, and T. Gozel, "Representative residential LV feeders: A case study for the North West of England," *IEEE Trans. Power Syst.*, vol. 31, no. 1, pp. 348–360, Jan. 2016.

[38] I. Richardson and M. Thomson, "Integrated simulation of photovoltaic micro-generation and domestic electricity demand: A one-minute resolution open-source model," *Proc. Inst. Mech. Eng. A, J. Power Energy*, vol. 227, no. 1, pp. 73–81, 2013.

[39] A. M. Blanco, E. Gasch, J. Meyer, and P. Schegner, "Web-based platform for exchanging harmonic emission measurements of electronic equipment," in *Proc. PIEEE 15th ICHQP*, 2012, pp. 943–948.

[40] E. McKenna and M. Thomson, "High-resolution stochastic integrated thermal–electrical domestic demand model," *Appl. Energy*, vol. 165, pp. 445–461, Mar. 2016. [Online]. Available: http://www.sciencedirect.com/science/article/pii/S0306261915016621

[41] M. F. McGranaghan, S. Santoso, R. C. Dugan, and H. W. Beaty, "Applied harmonics," in *Electrical Power Systems Quality*, 3rd ed. New York, NY, USA: McGraw-Hill Prof., 2012, pp. 255–324.

[42] A. Bosovic *et al.*, "Deterministic aggregated harmonic source models for harmonic analysis of large medium voltage distribution networks," *IET Gener. Transm. Distrib.*, vol. 13, no. 19, pp. 4421–4430, 2019.

[43] C. Debruyne, J. Desmet, and L. Vandevelde, "Estimation of end user voltage quality including background distortion," in *Proc. IEEE Power Energy Soc. Gen. Meeting*, 2012, pp. 1–7.

[44] D. B. Avancini, J. J. Rodrigues, S. G. Martins, R. A. L. Rabêlo, J. Al-Muhtadi, and P. Solic, "Energy meters evolution in smart grids: A review," *J. Clean. Prod.*, vol. 217, pp. 702–715, Apr. 2019. [Online]. Available: https://www.sciencedirect.com/science/article/pii/S0959652619302501

[45] Task force on Harrnonics Modeling and Simulation, "Modeling and simulation of the propagation of harmonics in electric power networks—Part I: Concepts, models, and simulation techniques," *IEEE Trans. Power Del.*, vol. 11, no. 1, pp. 452–465, Jan. 1996.

[46] G. G. Ye, M. M. Nijhuis, V. V. Cuk, and J. S. Cobben, "Stochastic residential harmonic source modeling for grid impact studies," *Energies*, vol. 10, no. 3, p. 372, 2017. [Online]. Available: https://www.narcis.nl/publication/RecordID/oai:library.tue.nl:866653

[47] P. Rodríguez-Pajarón, A. H. Bayo, and J. V. Milanović, "Probabilistic assessment of the influence of transformer rating on power quality indices in future residential networks," *Int. J. Electr. Power Energy Syst.*, vol. 135, Feb. 2022, Art. no. 107582. [Online]. Available: https://www.sciencedirect.com/science/article/pii/S0142061521008164

Pablo Rodríguez-Pajarón (Graduate Student Member, IEEE) received the B.S. and M.Sc. degrees in industrial engineering and the Ph.D. degree in electrical engineering from the Universidad Politécnica de Madrid, Madrid, Spain, in 2016, 2018, and 2022, respectively.

Araceli Hernández (Member, IEEE) is an Associate Professor with the Department of Automatics, Electrical and Electronics Engineering and Industrial Computing, Universidad Politécnica de Madrid, Madrid, Spain.

Jovica V. Milanović (Fellow, IEEE) is a Professor of Electrical Power Engineering and Deputy Head of Department with the Department of Electrical and Electronic Engineering, The University of Manchester, Manchester, U.K.